C.1

NATIONAL ADVISORY COMMITTEE FOR AERONAUTICS

TECHNICAL NOTE 3037

Instrumentation - Pulse Counting, etc

COUNTING METHODS AND EQUIPMENT FOR MEAN-VALUE MEASUREMENTS IN TURBULENCE RESEARCH

By H. W. Liepmann and M. S. Robinson

California Institute of Technology

Washington
October 1953

NATIONAL ADVISORY COMMITTEE FOR AERONAUTICS

TECHNICAL NOTE 3037

COUNTING METHODS AND EQUIPMENT FOR MEAN-VALUE MEASUREMENTS IN TURBULENCE RESEARCH

By H. W. Liepmann and M. S. Robinson

SUMMARY

This report deals with methods of measuring the probability distributions and mean values of random functions as encountered in turbulence research. Applications to the measurement of probability distributions of the axial velocity fluctuation $u(t)$ and its derivative du/dt in isotropic turbulence are shown. The assumption of independent probabilities of $u(t)$ and du/dt, which has been used as an approximation in the application of zero counts to the measurement of the microscale of turbulence λ, is investigated. The results indicate that the assumption is satisfied within a few percent and that there is, so far, no evidence that the systematic difference between λ measured from zero counts and λ measured independently can be traced entirely to the statistical dependence of u and du/dt.

The chronological development of apparatus is described, concluding with the present 10-channel statistical analyzer based upon a system of pulse amplitude modulation followed by an amplitude discriminator and a counter. A discussion of the relative merits of various systems is included to indicate the reasons for this choice.

INTRODUCTION

Let $I(x,y,z,t)$ represent a quantity such as a velocity component or a pressure in turbulent flow. Since turbulence is an essentially statistical phenomenon, $I(x,y,z,t)$ will not be representable in the same way as an ordinary function but will be defined only by certain probability distributions and mean values. Experimental studies of turbulent flow are thus primarily concerned with the measurement of mean values. There are several ways of defining the mean values of $I(x,y,z,t)$. Often the most convenient, theoretically, is to define $\overline{I}$ as an ensemble average; that is, one considers N similarly prepared systems, say wind tunnels with the same grid setup, and measures $I(x,y,z,t)$ simultaneously at corresponding points of these N wind tunnels. The N results can then be evaluated statistically and yield the probability distribution and the desired mean value.

Experimentally, and also often in theory, one uses instead the time average. One observes $I(x,y,z,t)$ for a sufficiently long time in one system and defines

$$\overline{I} = \frac{1}{T}\int_0^T I(x,y,z,t)\ dt$$

provided this is possible. If there exists a time-independent mean value, the integral will reach a constant value for a sufficiently large value of T. Clearly one can also use a space average, defined by

$$\overline{I} = \frac{1}{V}\iiint_V I(x,y,z,t)\ dx\ dy\ dz$$

where V is a certain volume in space. Finally, one can combine the latter two and average over both space and time.

Most of the recent experimental work in turbulent flow is concerned with flows which are steady in the mean, that is, for which the time average exists and for which the time and ensemble averages can be rigorously interchanged. Investigations of isotropic turbulence behind grids and of wakes, jets, channel flows, and so forth belong to this group. Isotropic turbulence set up in a box, on the other hand, is clearly a problem for which a time average has no meaning: here, evidently, the ensemble average or space average is wanted.

The mean value of a power of I, for example I^2 or I^3, can be measured in essentially three ways. First one can use a device which squares or cubes the instantaneous value of $I(x,y,z,t)$ and then proceed to take the desired mean value. Secondly one may use a device which produces the mean of a certain definite power directly, such as a thermocouple meter for measuring the time mean square of a current. Finally, one may obtain the probability distribution or probability density $p(\xi)$, where $p(\xi)\ d\xi$ denotes the probability of finding I between ξ and $\xi + d\xi$, and then obtain all the mean powers of I as the moments of $p(\xi)$. Whether a time or ensemble mean value results depends upon the determination of $p(\xi)$. If $p(\xi)\ d\xi$ denotes the fraction of time the function $I(x,y,z,t)$ spends between ξ and $\xi + d\xi$ divided by the total time T, a time average is taken. If $p(\xi)\ d\xi$ is defined as the number n of systems having values of I between ξ and $\xi + d\xi$ divided by the total number of systems, then an ensemble average is taken.

The methods described below are primarily intended for the measurement of time averages and are based on this last form of the averaging procedure. The original apparatus handled $p(\xi)$ directly, but it was subsequently found more convenient to work with the integrated probability density, or distribution function, $F(\xi)$, which is defined as the probability of finding $I(x,y,z,t)$ with a value greater than ξ and is related to the probability density as follows:

$$F(\xi) = \int_{\xi}^{\infty} p(\xi)\, d\xi \tag{1}$$

Clearly $F(-\infty) = 1$ and $F(\infty) = 0$. It follows that

$$dF = -p(\xi)\, d\xi \tag{2}$$

Although time averages are dealt with here, it is also possible to use the same procedures for ensemble averages.

The apparatus was built with the idea in mind of reducing the problem of finding the probability density, or the distribution function, to one of pulse counting. The advantages of such a procedure are that counting methods permit averaging over almost unlimited intervals of time, and pulse-counting circuits are in general very stable and satisfactory. This approach grew out of the investigation of the zeros of fluctuating-velocity components (ref. 1), reported earlier, which demonstrated the convenience of pulse-counting methods.

This work was carried out under the sponsorship and with the financial assistance of the National Advisory Committee for Aeronautics.

The authors wish to express their appreciation to Mr. George Skinner for his generous help in the preparation of the manuscript. The original gate apparatus was designed and built by Mr. C. Thiele and Dr. H. Wright, who furnished very useful advice during the early stages of the work. Part of the work reported here was done as early as 1949. The present report summarizes both the earlier work and recent developments (ref. 2).

SYMBOLS

t	time
ξ,η	amplitude coordinates
$u(t)$	axial velocity fluctuation

$V(t)$ any fluctuating input voltage with zero mean

λ microscale of turbulence

$p(\xi)$ probability density

$p(\xi,\eta)$ joint probability density

$F(\xi)$ distribution function

Dimensionless parameters:

$$C = \frac{\sqrt{\overline{v^2}}}{|\overline{v}|}$$

$$S = \frac{\overline{v^3}}{\left(\overline{v^2}\right)^{3/2}} = \text{Skewness}$$

$$f = \frac{\overline{v^4}}{\left(\overline{v^2}\right)^2} = \text{Flatness}$$

For a Gaussian distribution:

$$C = \sqrt{\frac{\pi}{2}}$$

$$S = 0$$

$$f = 3$$

PRINCIPLES OF APPARATUS

In all cases the apparatus handles a fluctuating voltage $V(t)$ (figs. 1(a) and 2(a)) such as the output of a hot-wire and amplifier combination. The term $V(t)$ may represent a velocity fluctuation measured at a certain point, its derivative, or so forth. The original experimental apparatus was set up to determine the statistical properties of $V(t)$ by measuring its probability density step by step, using a gate circuit essentially similar to Townsend's "statistical

analyzer" (ref. 3) which passes a signal only if the amplitude of $V(t)$ lies within a narrow range of voltages. Specifically this circuit produces a signal of constant amplitude during the time that $V(t)$ lies between ξ and $\xi + d\xi$, where ξ is the voltage setting of the gate. Hence the operation performed by the gate circuit yields a signal like the one shown in figure 1(b), consisting of irregularly spaced square waves of uniform height. The total area of these square waves, or the sum of all their widths, measured over a time interval T, thus gives the time T_1 which $V(t)$ spends between ξ and $\xi + d\xi$ during T. The probability density $p(\xi)\ d\xi$ is defined by stating that $p(\xi)\ d\xi$ denotes the fraction of T which $V(t)$ spends between ξ and $\xi + d\xi$; that is,

$$p(\xi)\ d\xi = \frac{T_1}{T} \tag{3}$$

To measure the sum of the widths of the square segments of figure 1(b), a counting method is used as follows: A pulse generator produces equidistant pulses at a rate of, say, M per second (fig. 1(c)). A coincidence circuit mixes the signals in figures 1(b) and 1(c), giving the result shown in figure 1(d). The signal in figure 1(d), which consists of a set of "chopped" square waves, is fed into a counting circuit. Let m be the number of counts obtained per second, then evidently

$$p(\xi)\ d\xi = \frac{m}{M} \tag{4}$$

Varying ξ then yields $p(\xi)$ completely. From $p(\xi)$ the averages are obtained as the moments; for example,

$$\overline{V^2} = \frac{\int \xi^2 p(\xi)\ d\xi}{\int p(\xi)\ d\xi}$$

$$\overline{V^3} = \frac{\int \xi^3 p(\xi)\ d\xi}{\int p(\xi)\ d\xi}$$

. . . . . .

The time over which a count is taken is evidently limited only by the stability of the whole setup. Especially important for large values of ξ, for which $p(\xi)$ is very small indeed, is the fact that the time of measurement can be increased and the accuracy very much improved.

This first method lends itself well to direct measurements of mean values by making use of Simpson's rule in determining how long to let the apparatus run at each value of ξ. This technique is described in the section "Obtaining Mean Values."

To reduce the measuring time involved, a number of gate circuits can be combined into a multichannel analyzer, so that $p(\xi)$ can be completely determined in one short run. However, when a multichannel arrangement is considered, it becomes evident that one should change to a system which measures $F(\xi)$ rather than $p(\xi)$. The reasons for this will be discussed in the sections "Details of Apparatus" and "Errors in Apparatus."

The principles of this multichannel form of the apparatus are illustrated in figure 2. Since the counting circuits require their information in the form of narrow pulses, the incoming signal $V(t)$ is first made to amplitude modulate a continuous train of pulses (fig. 2(b)) in such a way as to result in a pattern (fig. 2(c)) which lies completely above the zero voltage line. A discriminator, or rectifier, which is biased to a voltage value of ξ is then used to cut off any pulses whose height does not exceed ξ (fig. 2(d)). Sufficient amplification of those pulses which pass the discriminator is provided to insure that each will register in the counting circuit which follows. In the multichannel setup, 10 discriminators are used, each set at a different ξ level. These levels are adjustable to permit the use of all 10 channels for any portion of the incoming signal to obtain, for example, 10 points on the distribution function for positive values of $V(t)$ and 10 points for negative values of $V(t)$ by reversing the input signal.

It will be observed that in passing from $V(t)$ (fig. 2(a)) to the train of modulated pulses (fig. 2(c)) the zero level of the signal has been lost. This must be redetermined later using the knowledge that, by definition, $V(t)$ is a fluctuating voltage whose mean value is zero, giving a value ζ_0 which corresponds to $V(t) = 0$. One can then say

$$\xi = \zeta - \zeta_0 \tag{5}$$

If, again, the pulse generator supplies a train of pulses at the rate of, say, M per second (fig. 2(b)) and m is the number of counts obtained per second, then evidently

$$F(\xi) = \frac{m}{M} \tag{6}$$

OBTAINING MEAN VALUES

Direct Measurement

With the original gate circuit for measuring $p(\xi)$, it was possible to measure mean values directly, by the application of Simpson's rule; that is, the integration giving the appropriate moment of $p(\xi)$ could be carried out with the apparatus itself.

Assume that the pulse generator furnishes M pulses per second and that for a given value of ξ the count is taken over t_ξ seconds leading to a total of m_ξ pulses counted. Then:

$$p(\xi)\, d\xi = \frac{m_\xi}{Mt_\xi}$$

or

$$t_\xi p(\xi)\, d\xi = \frac{m_\xi}{M} \tag{7}$$

Assume now that the zero moment α_0, that is,

$$\alpha_0 = \int_{-\infty}^{\infty} p(\xi)\, d\xi$$

is to be measured. Using Simpson's rule the integral can be written as the sum

$$\int_0^{\infty} p(\xi)\, d\xi = \frac{1}{3}\left[p(0) + 4p(1) + 2p(2) + \ldots\right] \tag{8}$$

if the interval $\xi_n - \xi_{n-1}$ is put equal to 1 for convenience. Similarly the other part of the integral may be written

$$\int_{-\infty}^{0} p(\xi)\, d\xi = \frac{1}{3}\left[p(0) + 4p(-1) + 2p(-2) + \ldots\right] \tag{9}$$

Since $p(\xi)$ goes to zero for large values of $|\xi|$ it is irrelevant how the last point is chosen, provided the sum is extended to large enough values of $|\xi|$.

Consider equation (7) and choose t_ξ in such a way that $t_0 = \tau$, $t_{\pm 1} = 4\tau$, $t_{\pm 2} = 2\tau$, and so forth. Then clearly

$$\sum_{\xi=0,1,\ldots} m_\xi = M\tau\left[p(0) + 4p(1) + 2p(2) + \ldots\right]$$

that is,

$$\sum_{\xi=0,1,\ldots} m_\xi = 3M\tau \int_0^\infty p(\xi)\, d\xi \tag{10}$$

and similarly

$$\sum_{\xi=0,-1,\ldots} m_\xi = 3M\tau \int_{-\infty}^{0} p(\xi)\, d\xi \tag{11}$$

Thus if one sets the device successively to $\xi = 0, 1, 2, 3, \ldots$, counts time τ, 4τ, 2τ, . . . seconds, and leaves the numbers in the register, the apparatus performs the summation and by virtue of equation (10) the integration for positive values of ξ. By reversing the input the integration for negative values of ξ is obtained.

The procedure can be applied in principle to any moment integral α_n, since

$$\alpha_n = \int_{-\infty}^{\infty} \xi^n p(\xi)\, d\xi \qquad n = 1, 2, 3, 4, \ldots$$

Now t_ξ is chosen as follows:

$$t_0 = 0 \qquad t_{\pm 1} = 4\tau(\pm 1)^n \qquad t_{\pm 2} = 2\tau(\pm 2)^n \qquad \ldots$$

Thus

$$t_\xi p(\xi) = \begin{cases} \left.\begin{array}{ll} 2\tau\xi^n p(\xi) & n = 2,4 \\ 4\tau\xi^n p(\xi) & n = 1,3 \end{array}\right\} \xi > 0 \\ \left.\begin{array}{ll} 2\tau(-1)^n\xi^n p(\xi) & n = 2,4 \\ 4\tau(-1)^n\xi^n p(\xi) & n = 1,3 \end{array}\right\} \xi < 0 \end{cases} \tag{12}$$

and thus

$$\sum_{\xi>0} m_\xi = 3M\tau \int_0^\infty \xi^n p(\xi)\, d\xi \tag{13}$$

and

$$\sum_{\xi<0} m_\xi = (-1)^n 3M\tau \int_{-\infty}^0 \xi^n p(\xi)\, d\xi$$

A procedure like this is sometimes convenient. Since the functions are smooth, not very many points are required to approximate the integrals very closely. It is also evident that this procedure could well be performed automatically if the additional apparatus were warranted.

Short Cuts

For some applications it is possible to shorten the procedure very much by using a known form of $p(\xi)$. For example, assume that $V(t)$ represents a velocity fluctuation $u(t)$ in isotropic turbulence. In this case one knows that $p(\xi)$ is very nearly a Gaussian distribution. Thus:

$$p(\xi) = p(0)e^{-\frac{\xi^2}{2\overline{\xi^2}}}$$

and hence

$$p(\xi_1) = p(0)e^{-\frac{1}{2}\frac{\xi_1^2}{\overline{\xi^2}}}$$

Thus

$$\overline{u^2} \approx \overline{V^2} \equiv \overline{\xi^2} = \frac{\xi_1^2}{2 \log \frac{p(0)}{p(\xi_1)}} = \frac{\xi_1^2}{2 \log \left(\frac{m_0}{m_{\xi_1}}\right)} \tag{14}$$

and thus $\overline{\xi^2}$ is obtained as the ratio of two measurements. Similarly $\overline{\xi^4}$ can be obtained.

Computation of Mean Values Using Multichannel Analyzer

Consider the mean value of the nth power of the input $V(t)$:

$$\overline{V^n} = \frac{\int_{-\infty}^{\infty} \xi^n p(\xi)\, d\xi}{\int_{-\infty}^{\infty} p(\xi)\, d\xi}$$

Now

$$\int_{-\infty}^{\infty} p(\xi)\, d\xi = 1$$

so that

$$\overline{V^n} = \int_{-\infty}^{\infty} \xi^n p(\xi)\, d\xi$$

and by equations (1) and (2)

$$\overline{V^n} = \int_0^1 \xi^n \, dF$$

Because of the factor ξ^n, the integrand becomes infinite at the limits, making it unsuitable for numerical evaluation. This difficulty can be overcome by transforming to an integral with respect to the ξ-axis. Splitting the integral into two parts about $\xi = 0$:

$$\overline{V^n} = \int_0^a \xi^n \, dF + \int_a^1 \xi^n \, dF$$

$$= \int_0^a \xi^n \, dF - \int_{1-a}^0 \xi^n \, d(1 - F)$$

where $F(0) = a$. Integrating by parts:

$$\overline{V^n} = \left[\xi^n F\right]_{\xi=\infty}^{\xi=0} - \int_\infty^0 n\xi^{n-1} F \, d\xi - \left[\xi^n (1 - F)\right]_{\xi=0}^{\xi=-\infty} + \int_0^{-\infty} n\xi^{n-1}(1 - F) \, d\xi$$

or

$$\overline{V^n} = \left[\xi^n F\right]_{\xi=\infty}^{\xi=0} - \left[\xi^n (1 - F)\right]_{\xi=0}^{\xi=-\infty} + n\left[\int_0^\infty \xi^{n-1} F \, d\xi + \int_0^{-\infty} \xi^{n-1}(1 - F) \, d\xi\right]$$

The first two terms vanish at the limits if $F(n)$ approaches zero exponentially or faster as ξ approaches minus infinity. This requirement is always satisfied if the mean value is finite. Therefore

$$\overline{V^n} = n\left[\int_0^\infty \xi^{n-1} F \, d\xi + \int_0^{-\infty} \xi^{n-1}(1 - F) \, d\xi\right] \tag{15}$$

The integrals are evaluated numerically by Simpson's rule. (See fig. 3.) Since the main concern in turbulence work is distributions approaching a Gaussian form, the fourth moment of a Gaussian distribution was computed by Simpson's rule, using nine points. The result deviated from the theoretical value by less than 1 percent.

In practice, the normalization procedure

$$\int_{-\infty}^{\infty} p(\xi)\, d\xi = 1$$

involves dividing the number of counts m_ξ in any register by the total number of pulses generated by the pulse generator during the counting time M_0 so that:

$$\overline{V^n} = n\left[\int_0^{\infty} \xi^{n-1} \frac{m_\xi}{M_0}\, d\xi + \int_0^{-\infty} \xi^{n-1}\left(1 - \frac{m_\xi}{M_0}\right) d\xi\right] \tag{16}$$

One can conveniently run the generator for 1 minute with a pulse rate of 10^5 per minute, so that

$$\frac{m_\xi}{M_0} = \frac{m_\xi}{10^5}$$

Finally, it may be called to mind once again that the exact position of $\xi = 0$ is not known beforehand. Using the fact that the first moment of the distribution function is equal to zero (that is, $\overline{V} = 0$), the position of this axis may be determined. This procedure has proved more satisfactory than any in which one tries to set the initial "zero" pulse amplitude to some known arbitrary value with the accuracy required for computing mean odd powers.

DETAILS OF APPARATUS

Original Gate Circuit for $p(\xi)$

The circuit diagrams of the elements are shown in figures 4 and 5. The block diagram is given in figure 6, which should be self-explanatory.

The mixer will be seen to be a twin triode normally running saturated through a common anode load resistance. Strong negative grid signals will cut off the triodes, but a large anode signal will appear only when both halves of the tube are cut off simultaneously. The small effect of one-half being cut off alone is omitted in the block diagram. It should be pointed out that one-half of the first mixer receives a positive square wave which causes grid current to flow, thereby building up a steady negative bias nearly equal to the peak voltage of that square wave, so that it considers itself to be receiving a negative input during the periods when this positive square wave is absent. As the $\xi + d\xi$ line approaches the peak of the input signal, this positive square wave becomes of very short duration and it is difficult for the mixer to hold its bias. In operation the steps shown in figure 6 must be studied on an oscilloscope and levels adjusted, so that the sundry effects, such as those mentioned above, do not interfere with the counting of the desired pulses.

The signal is first amplified to about a 100-volt peak, to enable the gap to be of the order of a few volts and still be small compared with the peak amplitude. The Helipot A (fig. 4) adjusts the triggering point of the gate, that is, ξ; the two resistances B and C adjust the operating points of the two sides of the gate independently and hence set the gap width, that is, $d\xi$.

Adjustments are made by studying the output of the entire device on an oscilloscope, while a sine-wave signal is being fed in. The position of A for $\xi = 0$, the width of the gap $d\xi$ in volts, and the amplification factor giving ξ or the setting of A in volts can be determined in this fashion.

Pulses can be generated in any convenient manner, for example, by differentiating a square wave and suppressing the positive pulses produced, but for many applications it is quite good enough simply to use a sine wave. The frequency was ordinarily chosen to be 20 kilocycles per second, but different frequencies have been used.

The resulting pulse sequences are counted on a binary scalar counter feeding a mechanical register having a maximum rate of 60 per minute and capable of registering up to 10^4. The binary system is standard practice and uses diode coupling. The mechanical counter (a Cyclotron Specialities product) can be switched in to count every 2^5 to 2^9 pulse by tapping onto the output of the fifth, sixth, . . ., ninth stages of the binary scalar counter. This switching is useful in obtaining more counts on the register at low counting rates (in preference to reading the neon light of each stage and adding to the register reading) and may also be employed when integrating by Simpson's rule with the apparatus.

Multichannel Analyzer

In the section "Principles of Apparatus" the basic principles were outlined and these are shown pictorially in figure 2. The incoming signal V(t) (fig. 2(a)) is first added to a train of pulses, having a rise time of about 2 microseconds, obtained by differentiation of a square wave of frequency up to 10 kilocycles per second. Figure 7 shows an oscillogram of a single pulse, while figure 8 shows the sum of V(t) and the pulses, when V(t) is a sine wave. This step is accomplished by means of a differential amplifier (ref. 4), which handles an input of about 1 volt peak to peak across 1/2 megohm, at frequencies ranging from 1/2 to 50,000 cycles per second. By means of rectification and direct-current restoration, the lower part of the signal (fig. 8) is removed and the line A-A is made the zero level, leading to the result shown in figure 9, which has a maximum level of about 90 volts. The circuit diagram of the pulse amplitude modulator is shown in figure 10.

The modulated pulses are then fed into 10 amplitude discriminator channels each consisting of a biased diode (fig. 11) which passes that portion of any pulse which exceeds the bias voltage. For example, a 51-volt pulse will pass a discriminator biased to 50 volts as a pulse of 1-volt amplitude. The amplifier which follows each discriminator is capable of causing a 0.05-volt pulse to be counted, which corresponds to a sensitivity of better than 1 percent of the bias difference between adjacent channels. At present the bias levels are set by dry cells, but it is intended to replace these by a regulated power supply and a chain of precision resistors. To obtain intermediate bias settings (for example, if it is desired to double the number of points read, by making two runs) the diode bias ground tap may be shifted.

To minimize the effect of differences in the characteristics of the diodes they are heated by 3.9 volts instead of the usual 6 volts. This also reduces the quiescent plate currents.

Each channel is provided with from one to four commercial electronic decade scalars followed by a five-place impulse-type mechanical register. The decades operate on the "flip-flop" principle (ref. 5) and indicate their count by means of neon lights. The mechanical register is coupled to the last decade by means of a cathode follower and power amplifier. A maximum of 10^9 counts may be stored in each channel.

The analyzer may be used to study all, or only part, of an incoming signal according to where the modulator output is set relative to the discriminator voltages. When dealing with a complete distribution function, the input is disconnected and the modulator output (uniform pulses) is adjusted so that the middle channel just starts to count.

This, as has been explained, is not used as the zero level, which is determined later by computation. To count only one-half of the signal at a time, the same procedure is followed, except that the output is adjusted so that the lowest channel just starts to count. By reversing the input signal, the other half may be analyzed, giving a total of 20 points on the distribution curve.

A run is made by switching the modulator output to the amplitude discriminators for a measured time. For a 1-minute run the timing error is less than 1/2 percent.

ERRORS IN APPARATUS

Stability

In the original gate-circuit setup, stability was exceedingly important because of the measuring times involved (up to 2 hours in some cases). Long "warm-up" periods were essential, particularly to insure the stability of the $\xi = 0$ level, as this is of paramount importance in determining means from the odd moments of the probability-density curve since this involves a small difference between large numbers and is extremely sensitive to errors in the $\xi = 0$ setting. For example, the most important skewness factor in turbulent flow $\overline{(du/dt)^3}$ is obtained by measuring the distribution of du/dt, $p(\eta)$ say, and forming the integral

$$\int_{-\infty}^{\infty} \eta^3 p(\eta)\, d\eta = \int_{0}^{\infty} \eta^3 p(\eta)\, d\eta - \int_{0}^{-\infty} \eta^3 p(\eta)\, d\eta$$

either by computation or in the apparatus. The real difficulty arises because the relative position of the zero level of the incoming signal and the zero level of the gate or multichannel discriminators may change with time. In using the 10-channel analyzer for measuring $F(\xi)$, it was estimated that, in the case of the above skewness factor, a 3-percent error would arise if a constant error in the position of the $\xi = 0$ level of 1/2 percent of the interval between adjacent channels existed.

Generally one can achieve sufficient stability, particularly for the short times required for a run with the multichannel apparatus, and by computing the $\xi = 0$ axis from the first moment of the probability distribution or by equating areas of each half of the distribution function (see appendix) the error can be minimized, in the case of the multichannel setup, to 0.1 percent of the interval between channels.

Hysteresis

Any circuit designed to trigger at a certain voltage will exhibit a certain amount of hysteresis. Some hysteresis is necessary for stability. In effect, the circuit triggers at one voltage when the input is increasing and at a slightly lower voltage when the input is decreasing. The effect of this imperfection can be reduced by increasing the voltage of the input signal. However, too large an input signal results in a very short time of transit through the gap, in the case of the original gate circuit, and the final output square waves become distorted, making it impossible to count properly. In the case of the multichannel analyzer, the use of biased diodes as discriminators has reduced hysteresis to a negligible amount.

Gap Width in Original Gate Circuit

The finite width of the gap does introduce a correction, which, however, can be estimated. If the gate width is equal to ϵ, say, then what is really measured is the quantity

$$p(\xi)_{meas} = \frac{1}{\epsilon}\int_{\xi}^{\xi+\epsilon} p(\xi')\, d\xi' \tag{17}$$

and not $p(\xi)\, d\xi = p(\xi)\epsilon$. For a small ϵ, however, one evidently has

$$\int_{\xi}^{\xi+\epsilon} p(\xi')\, d\xi' = p(\xi)\epsilon + p'(\xi)\,\frac{\epsilon^2}{2} + \ldots \approx p(\xi)\epsilon\left(1 + \frac{p'}{p}\,\frac{\epsilon}{2} + \ldots\right)$$

and for a known distribution the correction can be evaluated. For example, if $p(\xi)$ is nearly Gaussian

$$\int_{\xi}^{\xi+\epsilon} p(\xi)\, d\xi = p(\xi)\epsilon\left(1 - \frac{|\xi|\epsilon}{2\xi^2} + \ldots\right) \tag{18}$$

Ordinarily measurements have to be taken up to values of ξ of the order of $3\sqrt{\overline{\xi^2}}$. Hence the maximum error near the outer edges of the distribution is of the order

$$\frac{p(\xi)_{meas}}{p(\xi)} \approx 1 - \frac{3}{2}\frac{\epsilon}{\sqrt{\overline{\xi^2}}}$$

This error may be appreciable if fairly large gate widths are used. However, the errors in the dimensionless ratios of moments of $p(\xi)$, namely, the skewness and flatness factors, are much smaller and for the most part negligible. For example, the errors in the flatness factors can be evaluated from

$$p(\xi)_{meas} \approx p(\xi)\left(1 - \frac{\epsilon|\xi|}{2\overline{\xi^2}}\right) \tag{19}$$

The flatness factor f is

$$f = \frac{\int_{-\infty}^{\infty} \xi^4 p(\xi)\, d\xi}{\left[\int_{-\infty}^{\infty} \xi^2 p(\xi)\, d\xi\right]^2} \int_{-\infty}^{\infty} p(\xi)\, d\xi = \frac{\overline{\xi^4}}{\left(\overline{\xi^2}\right)^2} \tag{20}$$

The factor $\overline{f}$ obtained from the measured distribution can be written

$$\overline{f} = f \frac{\left(1 - \frac{\epsilon}{2\overline{\xi^2}} \frac{\int_0^{\infty} \xi^5 p\, d\xi}{\int_0^{\infty} \xi^4 p\, d\xi}\right)\left(1 - \frac{\epsilon}{2\overline{\xi^2}} \frac{\int_0^{\infty} \xi p\, d\xi}{\int_0^{\infty} p\, d\xi}\right)}{\left[1 - \frac{\epsilon}{2\overline{\xi^2}} \frac{\int_0^{\infty} \xi^3 p(\xi)\, d\xi}{\int_0^{\infty} \xi^2 p(\xi)\, d\xi}\right]^2} \tag{21}$$

In the correction term a Gaussian distribution can be used and since

$$\frac{\int_0^\infty \xi^n e^{-\beta^2\xi^2}\, d\xi}{\int_0^\infty \xi^{n-1} e^{-\beta^2\xi^2}\, d\xi} = \beta^{-1}\,\frac{\Gamma\left(\frac{n+1}{2}\right)}{\Gamma\left(\frac{n}{2}\right)} \tag{22}$$

it follows that

$$\bar{f} \approx f\left(1 + \frac{1}{3\sqrt{2\pi}}\,\frac{\epsilon}{\sqrt{\overline{\xi^2}}}\right)$$

$$= f\left(1 + 0.133\,\frac{\epsilon}{\sqrt{\overline{\xi^2}}}\right)$$

Hence even if the gate width ϵ is as large as 20 percent of $\sqrt{\overline{\xi^2}}$ the error in f is small.

Values for Multichannel Analyzer

As has been mentioned, the amplitude discrimination is reliable to 0.05 volt while the maximum pulse amplitude is about 90 volts. The amplifiers driving the decade counters can be trimmed for gain, so that when all are tied to the same level their readings will not deviate more than 1/2 percent from each other. Without trimming they are already good to 1 percent.

Using dry cells to set the discriminator levels, a spacing of $7\frac{1}{2}$ volts between channels can be maintained uniform to $1\frac{1}{2}$ percent accuracy with negligible drift over a period of a few months.

The zero level, as was explained earlier, can be computed to 0.1 percent of the interval between channels.

Over-all repeatability has been checked for a sine-wave input and found to be ±0.1 percent of the reading at each level. Measurements

of du/dt in a turbulent air stream gave the following scatter of the mean values computed from consecutive 1-minute runs:

$$|\overline{v}| \approx \pm 1 \text{ percent} \qquad \overline{v^2} \approx \pm 2 \text{ percent}$$

$$\overline{v^3} \approx \pm 3 \text{ percent} \qquad \overline{v^4} \approx \pm 4 \text{ percent}$$

Main Improvement Introduced by 10-Channel Setup

It should now be clear that, whereas the gate circuit draws its information from selected narrow bands of the incoming signal, the 10-channel device utilizes the whole signal. This can, of course, be done with the gate circuit by using only one trigger circuit and suitably rearranging the block diagram of figure 6, but, because of the long time involved in measuring, the stability requirements become prohibitive. Operating 10 channels as a $p(\xi)$ device with large intervals defeats the advantage of using $p(\xi)$, namely that moments can be computed in the apparatus by suitable timing (see section "Obtaining Mean Values"), since the correction outlined above in "Gap Width in Original Gate Circuit" has to be applied and therefore leads to computation work. It will be realized, too, that measuring $F(\xi)$ instead of $p(\xi)$ leads to certain simplifications in circuitry since each channel has to distinguish only whether each pulse does or does not rise above its bias level. These were the considerations which led to the adoption of the present arrangement.

Other schemes will be found in references 6 to 9, but the present arrangement is designed for relatively high counting rates.

SAMPLE APPLICATIONS

Sine Wave

The multichannel analyzer was checked out on a sine wave (190 cycles per second). The results for one-half of the signal are shown in figure 12, together with the theoretical result, and show close agreement.

Isotropic Turbulence

Figure 13 shows the results of measurements of $p(\xi)$ with the gate circuit, for the axial velocity distribution in isotropic turbulence behind a grid. The Gaussian distribution is shown for comparison.

Agreement is good and confirms observations by others, especially Townsend. Skewness and flatness factors are shown in the table in the next section.

Figure 14 shows $F(\xi)$ for the same quantity under practically the same conditions, as measured on the 10-channel analyzer.

Isotropic Turbulence, du/dt and d^2u/dt^2

Figure 15 presents the results of measurements of the distribution $p(\eta)$ of the velocity derivative du/dt, using the gate, while figure 16 presents the distribution function $F(\eta)$ for the same quantity and practically the same conditions. The interesting fact here is the asymmetry of the distribution as first demonstrated by Townsend (ref. 3). From the distribution $p(\eta)$ the mean values can be computed. However, in order to compute the odd moments, that is, du^3/dt for example, one has to be very sure about the origin of the coordinate η, that is, about the zero position. Since a stationary process is dealt with here, evidently

$$\frac{du}{dt} = \frac{\int_{-\infty}^{\infty} \eta p(\eta)\, d\eta}{\int_{-\infty}^{\infty} p(\eta)\, d\eta} = 0$$

Hence one has to obtain first the "center of gravity" of the distribution and then compute the moments about this point. For the even moments this is not very important and a slight shift of the zero point amounts to a negligible error. The details of the computation for the case of the 10-channel analyzer are given in the appendix.

The skewness and flatness factors obtained are shown in the following tables. Included also is the factor C defined by

$$C = \frac{\sqrt{\overline{u^2}}}{|\overline{u}|}$$

$$= \frac{\sqrt{\overline{\left(\frac{du}{dt}\right)^2}}}{\left|\overline{\frac{du}{dt}}\right|}$$

for u and du/dt, respectively. Results for d^2u/dt^2 using the 10-channel analyzer are also given. (Also see fig. 17.)

The following tables give a comparison of measurements behind a turbulence grid with a mesh size M = 3/4 inch; R_M denotes the Reynolds number based on the mesh size, and X/M denotes the dimensionless distance from the grid position.

With gate circuit, R_M = 8,100, and X/M = 62:

	S	f	C
u	0.002	2.56	$0.944\sqrt{\pi/2}$
du/dt	-0.42	3.76	$1.02\sqrt{\pi/2}$

With 10-channel analyzer, R_M = 11,000, and X/M = 50:

	S	f	C
u	0.006	2.73	$0.980\sqrt{\pi/2}$
du/dt	-0.439	3.80	$0.984\sqrt{\pi/2}$
d^2u/dt^2	0.031	4.59	$1.04\sqrt{\pi/2}$

These values agree well with Townsend's measurements. Townsend gives for the skewness factor of du/dt, S = -0.39, but the measurements plotted, for example in figure 8 of reference 10, range between 0.39 and 0.50 at least. The flatness factor of u found here is somewhat less than Townsend's value of 2.9 (ref. 11). Hence the present measurements do not agree as well with a Gaussian distribution, for which f = 3. The same result is borne out by C which should be $\sqrt{\pi/2}$ for a Gaussian distribution. Again the distribution of u does give a noticeable difference. The symmetry of the u distribution is, however, well shown by S, which is zero to a close approximation.

Joint Probability Density $p(\xi,\eta)$ From Zero Counts

During the investigation of the possibilities of using the number of zeros of u(t) to determine $\overline{(du/dt)^2}$ (or λ) it was necessary to assume that u(t) and du/dt were statistically independent; that is,

it was assumed that $p(\xi,\eta) = p_0(\xi)p_1(\eta)$. Using the present device with the original gate circuit it is possible to check how closely this assumption agrees with the facts, that is, how accurately $\overline{(du/dt)^2}$ can be measured from the zero counts.

The number $N(\xi)$ of ξ values of $u(t)$, that is, the number of times per second that $u(t)$ passes ξ, is given by (refs. 1 and 12)

$$N(\xi) = \int_{-\infty}^{\infty} |\eta| p(\xi,\eta)\, d\eta \tag{23}$$

Denote the probability distribution of $u(t)$, that is, the average time that $u(t)$ spends between ξ and $\xi + d\xi$, as $p_0(\xi)\, d\xi$. Evidently $p_0(\xi)$ can be written

$$p_0(\xi) = \int_{-\infty}^{\infty} p(\xi,\eta)\, d\eta$$

Taking the ratio N/p_1 one has

$$\frac{N(\xi)}{p_0(\xi)} = \frac{\int_{-\infty}^{\infty} |\eta| p(\xi,\eta)\, d\eta}{\int_{-\infty}^{\infty} p(\xi,\eta)\, d\eta} \tag{24}$$

Equation (24) describes the following facts: $p_0(\xi)\, d\xi$ denotes the time t which $u(t)$ spends between ξ and $\xi + d\xi$, and $N(\xi)$ gives the number of passages through ξ per unit time; hence the ratio

$$\frac{p_0(\xi)\, d\xi}{N(\xi)} = \tau$$

gives the average time of a single passage. Hence the average absolute slope of a passage is given by

$$|\overline{\eta}|_{\xi} = \frac{d\xi}{\tau} = \frac{N(\xi)}{p_0(\xi)}$$

In general, $|\overline{\eta}|_{\xi}$ will depend upon ξ; however, if $p(\xi,\eta) = p_0(\xi)p_1(\eta)$ then

$$\frac{N(\xi)}{p_0(\xi)} = \frac{\int_{-\infty}^{\infty} |\eta| p_1(\eta)\, d\eta}{\int_{-\infty}^{\infty} p_1(\eta)\, d\eta} = |\overline{\eta}| \tag{25}$$

which is independent of ξ. This relation means that, if the probabilities of u and du/dt are independent, the absolute mean of du/dt is the same at every point of the trace u(t).

An example for which this is evidently not true is a simple harmonic wave of angular frequency ω; that is

$$u(t) = \sin \omega t$$

Here, $N(\xi) = \omega/\pi$ is of course independent of ξ. However, the time spent between ξ and $\xi + d\xi$ increases with ξ and hence

$$\frac{N(\xi)}{p_0(\xi)} \longrightarrow 0 \quad \text{if} \quad \xi \longrightarrow 1$$

expressing the fact that the mean absolute slope $|\overline{\eta}|$ has its maximum at $\xi = 0$ and decreases to zero as $\xi \longrightarrow 1$.

Without any assumption on the joint probability $p(\xi,\eta)$ the mean absolute value of η can be written

$$|\overline{\eta}| = \frac{\iint_{-\infty}^{\infty} p(\xi,\eta)|\eta| \, d\xi \, d\eta}{\iint_{-\infty}^{\infty} p(\xi,\eta) \, d\xi \, d\eta}$$

or

$$|\overline{\eta}| = \frac{\int_{-\infty}^{\infty} N(\xi) \, d\xi}{\int_{-\infty}^{\infty} p_0(\xi) \, d\xi} \tag{26}$$

From a measured distribution of $N(\xi)$ and of $p_0(\xi)$ both the ratio in equation (24) and $|\overline{\eta}|$ according to equation (26) can be obtained and compared. The result is plotted in figure 18; N/p_0 at $\xi = 0$ is normalized to 1. If u and du/dt were strictly statistically independent $N(\xi)/p_0(\xi)$ would be constant and would agree with the ratio of the integrals in equation (26). Actually $N(\xi)/p_0(\xi)$ is not quite constant but shows a definite minimum and maximum, as seen in figure 18, and the ratio of the integrals is less than unity. At large values of ξ the errors in N/p_0 evidently become very large indeed since the ratio approaches 0/0. Still it is evident that N/p_0 does not vary much over the most important range of ξ near zero where $p_0(\xi)$ is large. The general behavior of N/p_0 is quite interesting and should be studied further. The error in using the value of $N(0)$ to determine $|\overline{\eta}|$ is quite small as seen from figure 18 (namely, 1 - 0.98 = 0.02).

There remains one other correction which has to be applied to λ measurements from zero counts. Evidently the zero counts furnish directly only the mean slope of u(t), that is, $|\overline{du/dt}|$. On the other hand λ is directly related to $\sqrt{\overline{(du/dt)^2}}$. Hence one has to relate $|\overline{du/dt}|$ to $\sqrt{\overline{(du/dt)^2}}$. In the simplest formulation one assumes $p_1(\eta)$

to be Gaussian and then the ratio

$$\left|\overline{\frac{du}{dt}}\right| = \sqrt{\frac{2}{\pi}}\sqrt{\overline{\left(\frac{du}{dt}\right)^2}}$$

Now $p_1(\eta)$ is not quite Gaussian and hence the relation between $|\overline{du/dt}|$ and $\sqrt{\overline{(du/dt)^2}}$ will differ from $\sqrt{2/\pi}$. Let

$$\left|\overline{\frac{du}{dt}}\right| = \frac{1}{C}\sqrt{\overline{\left(\frac{du}{dt}\right)^2}}$$

Then the formula employed in the measurement of λ by counting zeros should read

$$N^2(0) = \frac{U^2}{C^2 2\pi\lambda^2}$$

where U denotes the mean speed. For $C = \sqrt{\pi/2}$ the formula evidently reduces to the one used in reference 1

$$N^2(0) = \frac{U^2}{\pi^2\lambda^2} \tag{27}$$

The factor C was evaluated from the measured distribution $p_1(\eta)$ as has been shown in the preceding table:

$$\frac{1}{C} = 0.97$$

and hence

$$N^2(0) = 0.94\,\frac{U^2}{\pi^2\lambda^2} \tag{28}$$

Consequently in λ^2 about 6 percent error results from the use of the simple formula, equation (27). Thus λ would come out too large using equation (27). This is an error in the right direction since the measurements of references 1 and 13 consistently give too large values of λ as calculated from equation (27). The correction due to the weak statistical dependency of u and du/dt is, however, in the other direction and the combined effect of these two errors is insufficient to explain the differences found in reference 13 between λ from zero counts and λ measured independently. It seems more likely that these differences can be traced to small systematic errors in the equipment, for example, insufficient resolution.

Vortex Street

Figure 19 shows the distribution function, by the 10-channel analyzer, obtained in a vortex street behind a cylinder at a Reynolds number of 100. The hot-wire output was a very stable, almost triangular wave. A true triangular wave would give a straight-line distribution function. The rounded peaks of the actual wave form give deviations from a straight line near the ends, where the distribution curves inward as in the distribution function for the sine wave. This work was done in conjunction with the study of wakes (ref. 14).

California Institute of Technology,
Pasadena, Calif., September 29, 1952.

APPENDIX

CALCULATION OF POSITION OF $\xi = 0$ AXIS

Figure 20 is to be used in conjunction with this discussion of the calculation of the $\xi = 0$ axis. The distance ϵ of the zero axis from channel 5 is found by the following method.

For zero average value of the input signal,

$$A_1 + a_1 = A_2 + a_2$$

$$a_2 - a_1 = A_1 - A_2$$

where A_1 and A_2 are determined from the data by use of Simpson's rule.

The curve between channels 5 and 6 can usually be accurately approximated by a straight line. Therefore, a_1 and a_2 are computed by using the trapezoidal rule as follows:

$$a_1 = \frac{1}{2}(h_1 + l_1)\epsilon$$

$$a_2 = \frac{1}{2}(h_2 + l_2)(1 - \epsilon)$$

$$2(a_2 - a_1) = h_2 + l_2 - (h_1 + h_2)\epsilon - (l_1 + l_2)\epsilon$$

$$= h_2 + l_2 - (h_1 + h_2 + 1)\epsilon$$

But,

$$l_1 = h_1 + (1 - h_2 - h_1)\epsilon$$

$$l_2 = 1 - l_1$$

Substituting,

$$2(a_2 - a_1) = h_2 + 1 - h_1 + (h_1 + h_2 - 1)\epsilon - (h_1 + h_2)\epsilon - \epsilon$$

$$2(A_1 - A_2) = h_2 - h_1 + 1 - 2\epsilon$$

Therefore,

$$\epsilon = \frac{h_2 - h_1 + 1}{2} - (A_1 - A_2)$$

REFERENCES

1. Liepmann, H. W.: Die Anwendung eines Satzes über die Nullstellen stochastischer Funktionen auf Turbulenzmessungen. Helvetica Physica Acta, vol. 22, no. 2, Mar. 18, 1949, pp. 119-126.

2. Robinson, Martin S.: A Ten Channel Statistical Analyzer for Use in Turbulence Research. Aero. Eng. Thesis, C.I.T., 1952.

3. Townsend, A. A.: The Measurement of Double and Triple Correlation Derivatives in Isotropic Turbulence. Proc. Cambridge Phil. Soc., vol. 43, pt. 4, Oct. 1947, pp. 560-570.

4. Seely, Samuel: Electron-Tube Circuits. First ed., McGraw-Hill Book Co., Inc., 1950.

5. Chance, Britton, et al., eds.: Waveforms. First ed., McGraw-Hill Book Co., Inc., 1949.

6. Parsons, J. H.: Electronic Classifying, Cataloging, and Counting Systems. Proc. Inst. Radio Engs., vol. 37, no. 5, May 1949, pp. 564-568.

7. Westcott, C. H., and Hanna, G. C.: A Pulse Amplitude Analyzer for Nuclear Research Using Pretreated Pulses. Rev. Sci. Instr., vol. 20, no. 3, Mar. 1949, pp. 181-188.

8. Freundlich, H. F., Hinks, E. P., and Ozeroff, W. J.: A Pulse Analyzer for Nuclear Research. Rev. Sci. Instr., vol. 18, no. 2, Feb. 1947, pp. 90-100.

9. Wells, F. H.: A Fast Amplitude Discriminator and Scale-of-Ten Counting Unit for Nuclear Work. Jour. Sci. Instr., vol. 29, no. 4, Apr. 1952, pp. 111-115.

10. Batchelor, G. K., and Townsend, A. A.: Decay of Vorticity in Isotropic Turbulence. Proc. Roy. Soc. (London), ser. A, vol. 190, no. 1023, Sept. 9, 1947, pp. 534-550.

11. Batchelor, G. K., and Townsend, A. A.: The Nature of Turbulent Motion at Large Wave-Numbers. Proc. Roy. Soc. (London), ser. A, vol. 199, no. 1057, Oct. 25, 1949, pp. 238-255.

12. Rice, S. O.: Mathematical Analysis of Random Noise. The Bell System Tech. Jour., vol. 23, no. 3, July 1944, pp. 282-332; vol. 24, no. 1, Jan. 1945, pp. 46-108.

13. Liepmann, H. W., Laufer, J., and Liepmann, Kate: On the Spectrum of Isotropic Turbulence. NACA TN 2473, 1951.

14. Roshko, A.: On the Development of Turbulent Wakes From Vortex Streets. Ph. D. Thesis, C.I.T., 1952. (Also available as NACA TN 2913.)

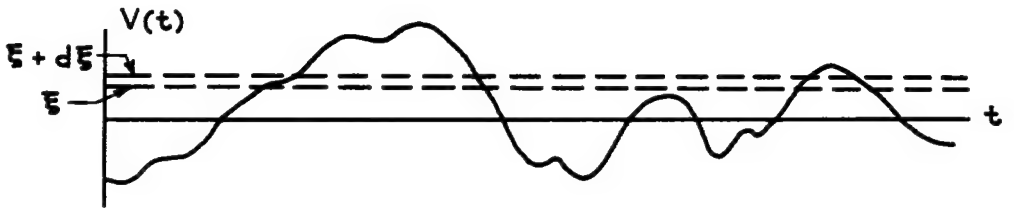

(a) Fluctuating voltage.

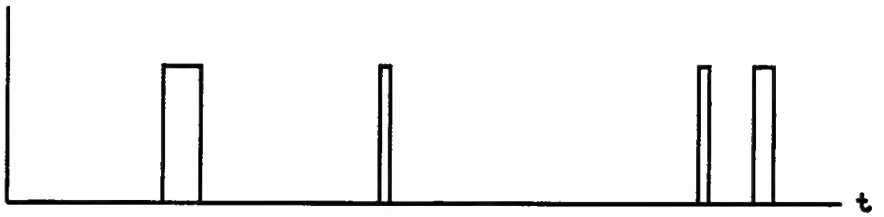

(b) Square-wave signal from gate circuit.

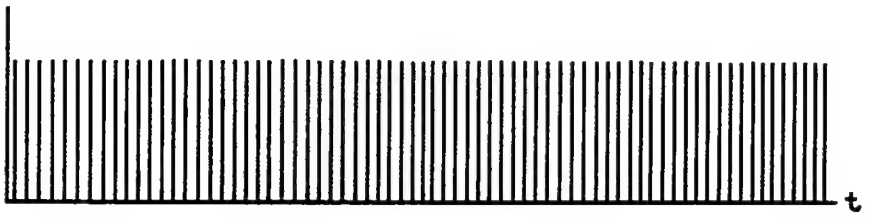

(c) Signal from pulse generator.

(d) Signal produced by mixing signals from gate and pulse-generator circuits.

Figure 1.- Principle of gate circuit.

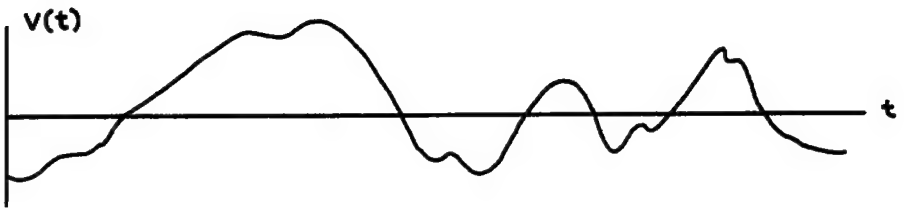

(a) Fluctuating voltage.

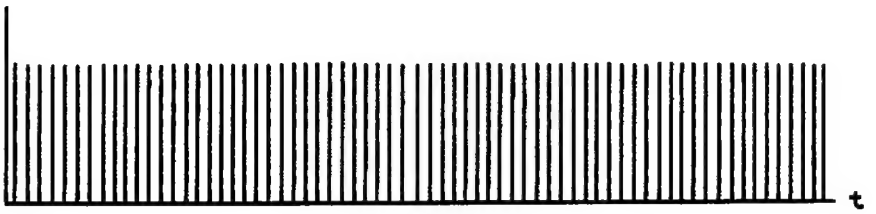

(b) Unmodulated pulses.

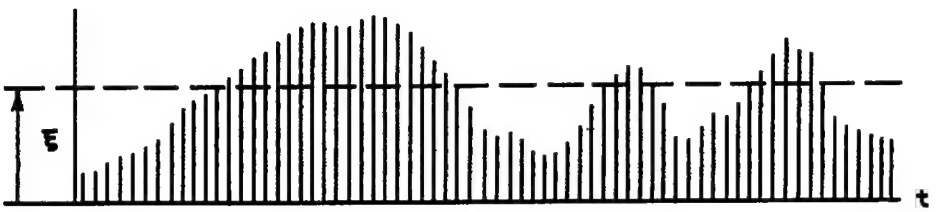

(c) Modulated pulses.

(d) Wave pattern from discriminator.

Figure 2.- Principle of 10-channel analyzer.

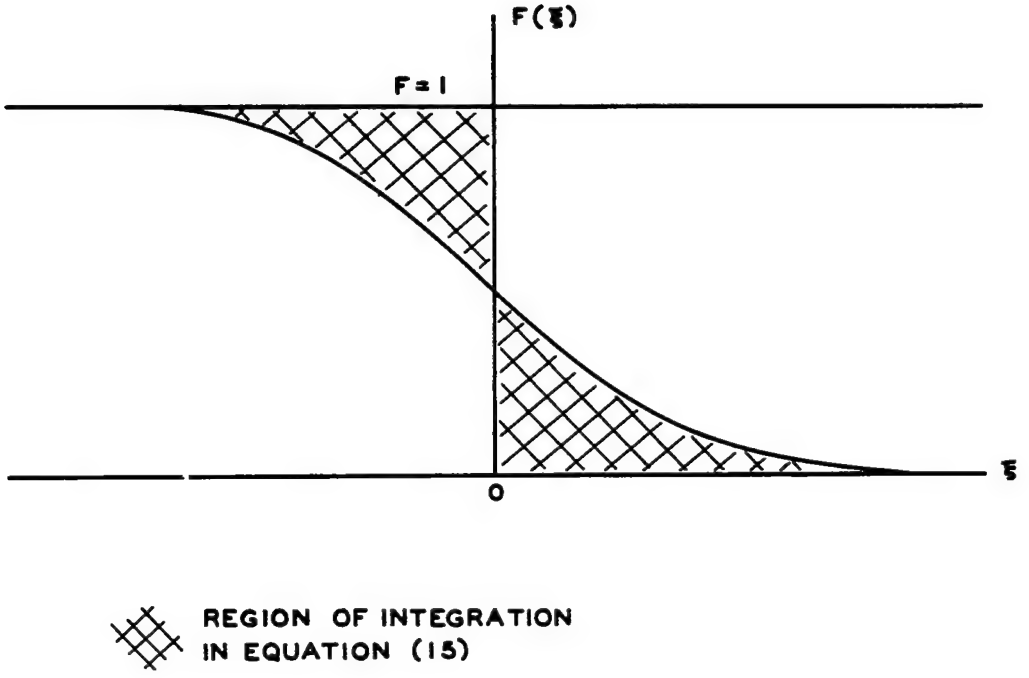

Figure 3.- Typical distribution function.

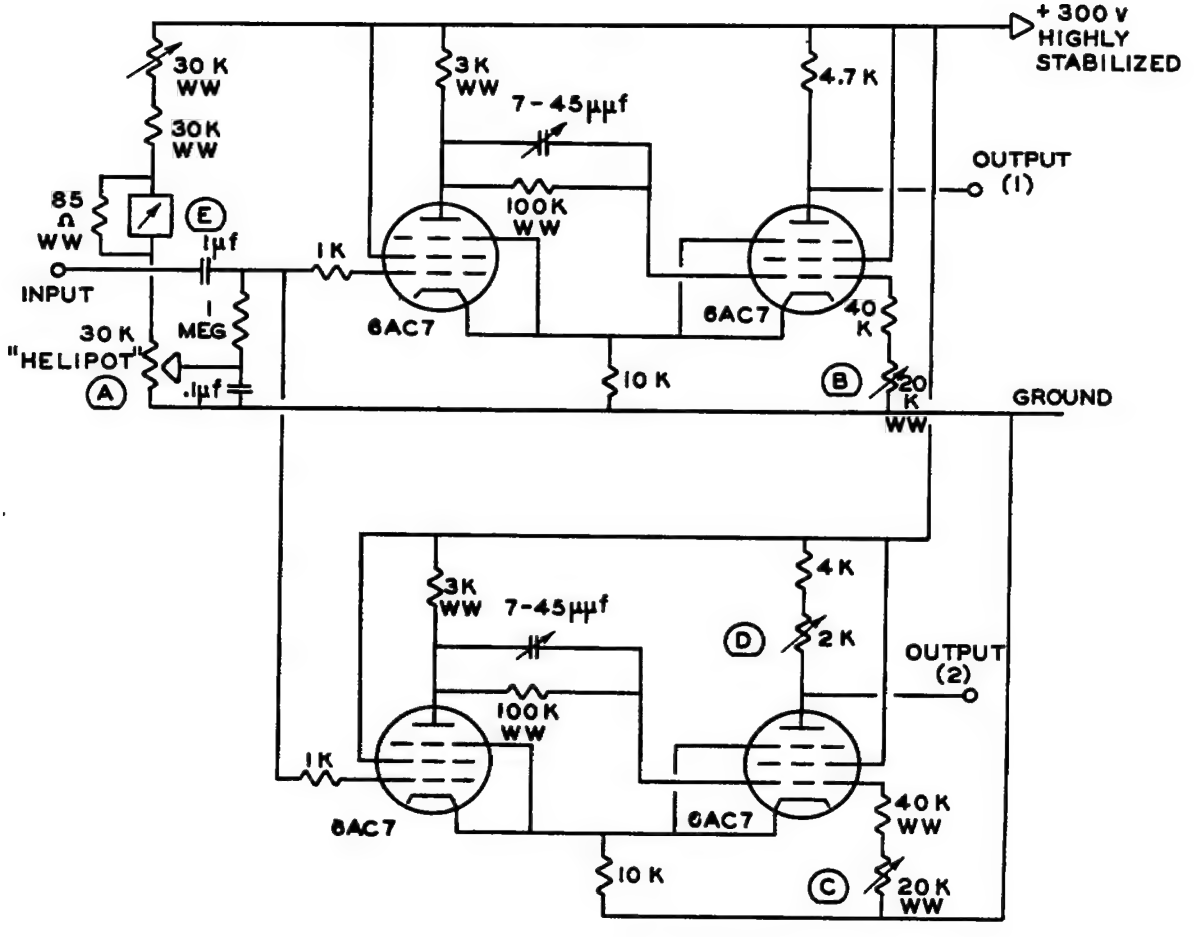

Figure 4.- Double-trigger circuit of gate. (K indicates thousand; WW, wire-wound resistor.)

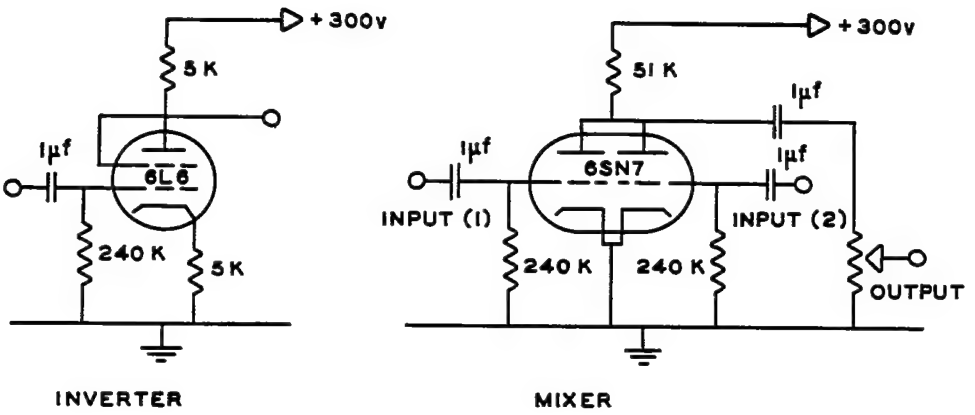

Figure 5.- Circuit diagrams of inverter and mixer. (K indicates thousand.)

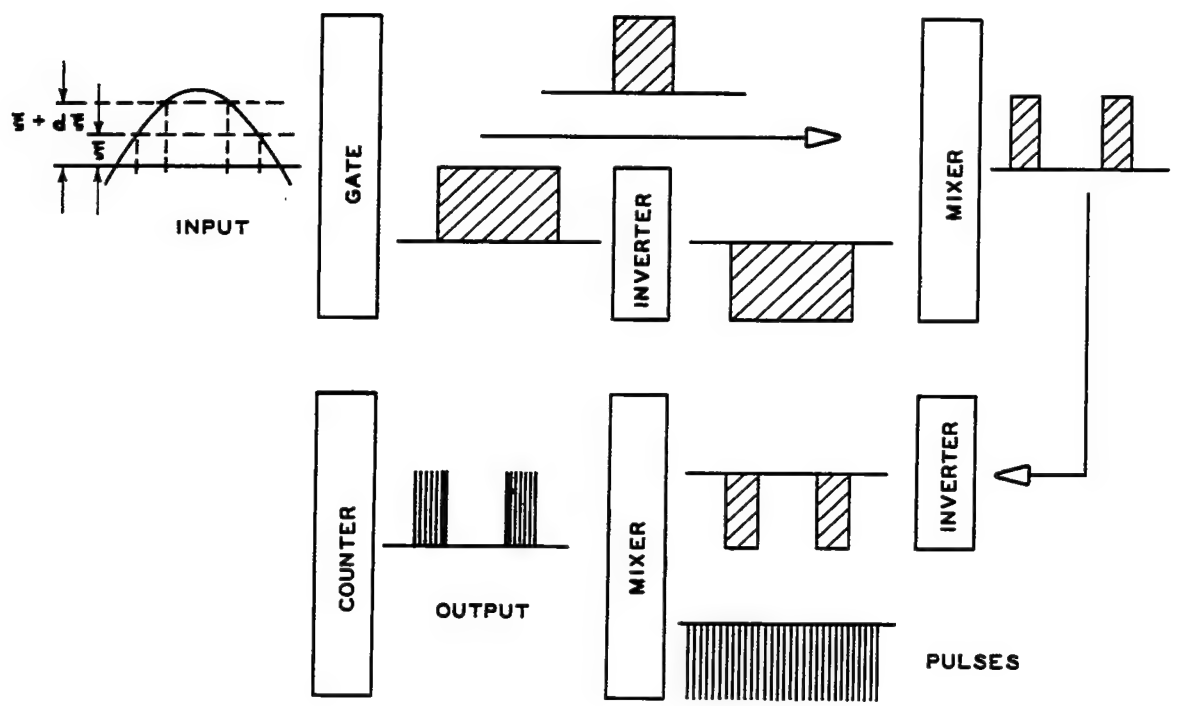

Figure 6.- Block diagram of apparatus.

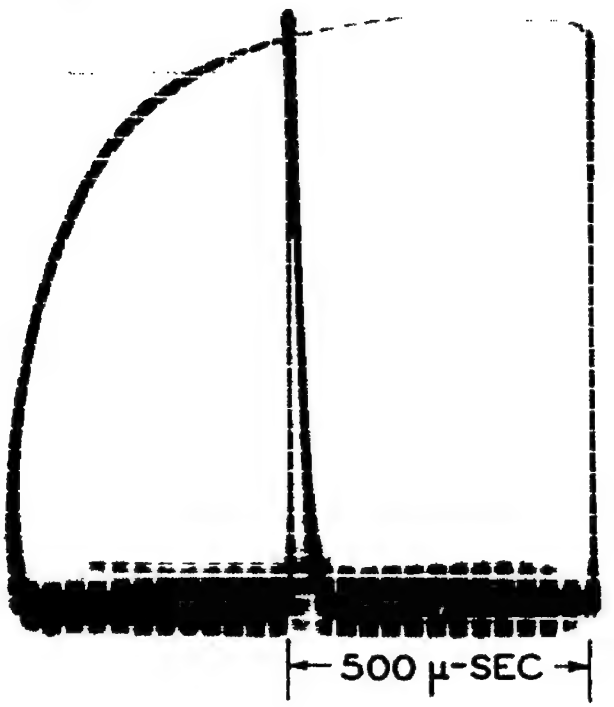

L-80245

Figure 7.- View of a single pulse.

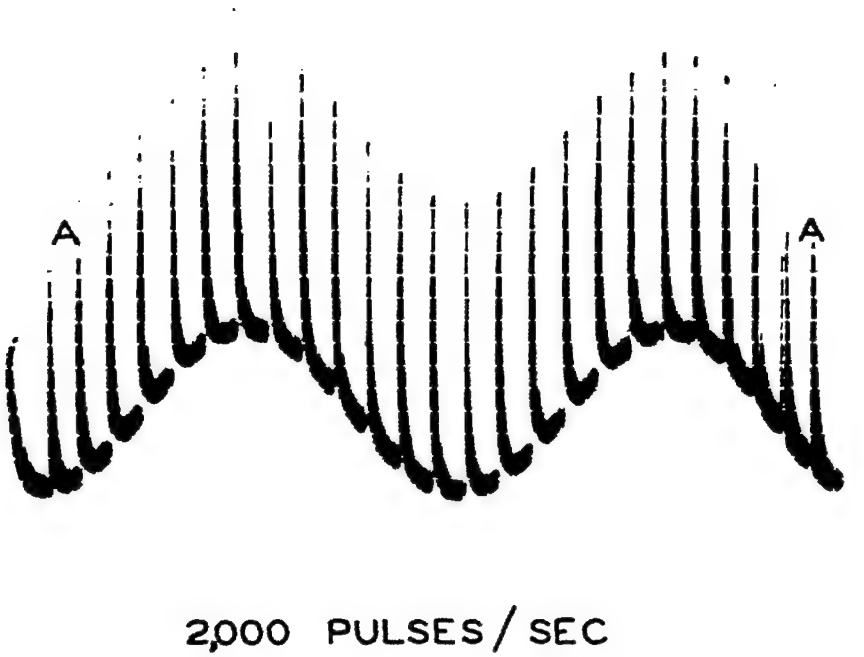

L-80246

Figure 8.- Differential amplifier output for a sine-wave input.

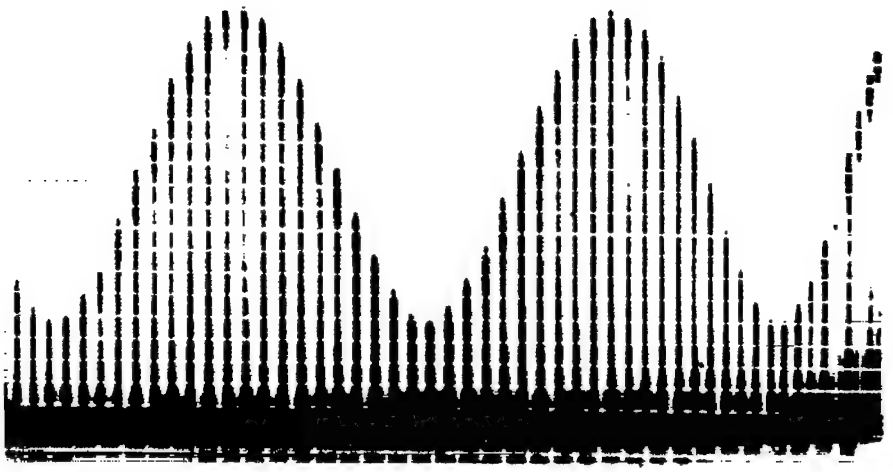

L-80247

Figure 9.- Modulator output for a sine-wave input.

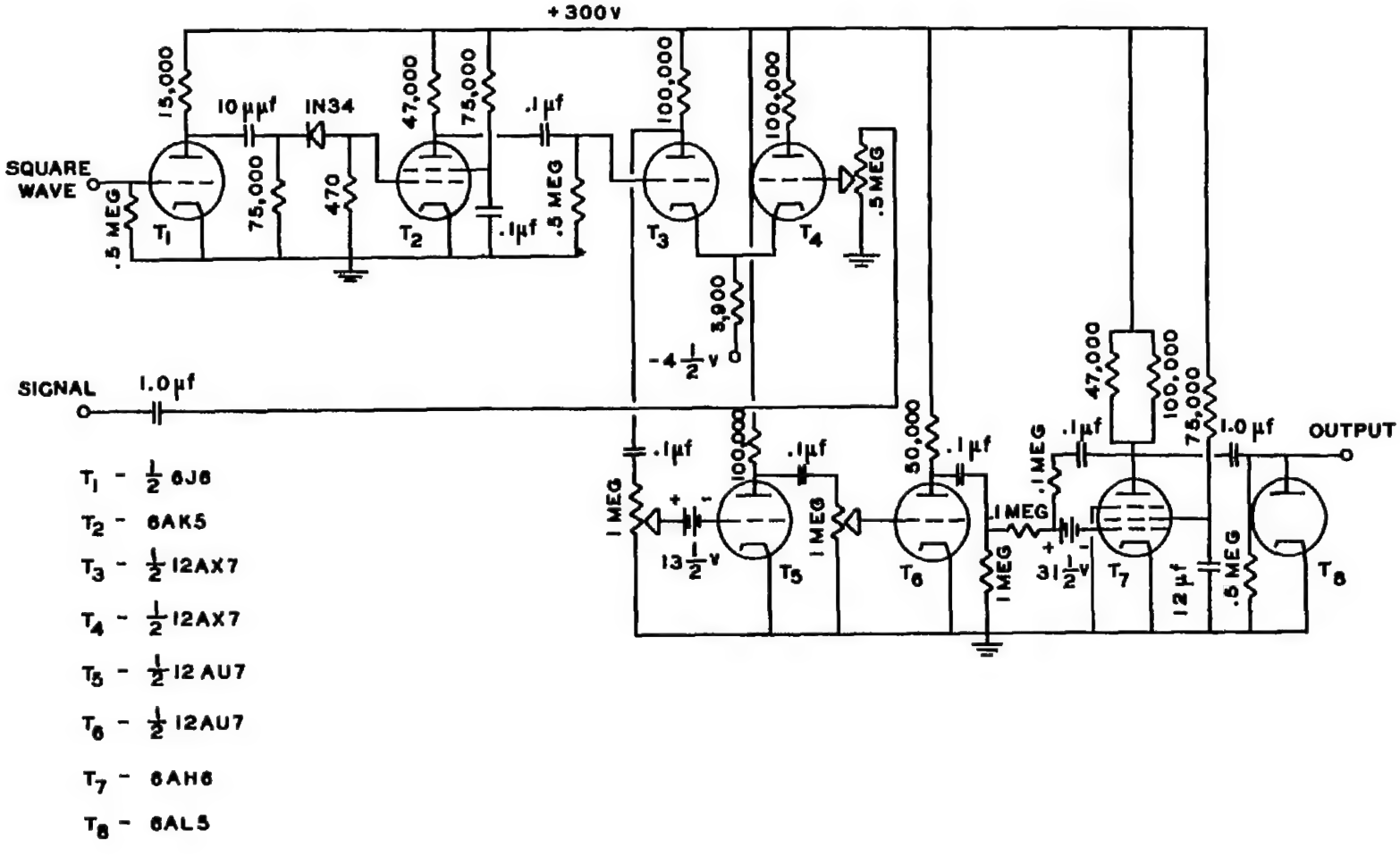

Figure 10.- Circuit diagram of pulse amplitude modulator.

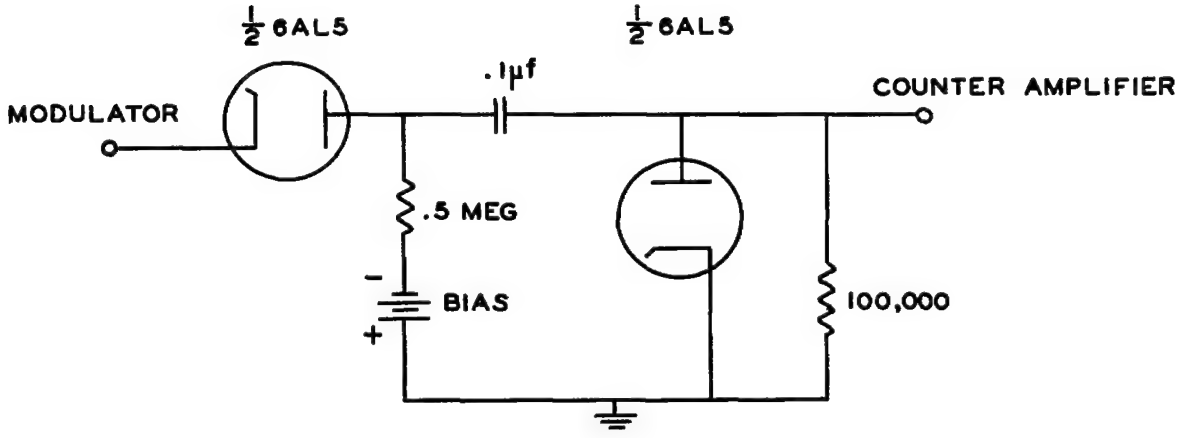

Figure 11.- Pulse height discriminator.

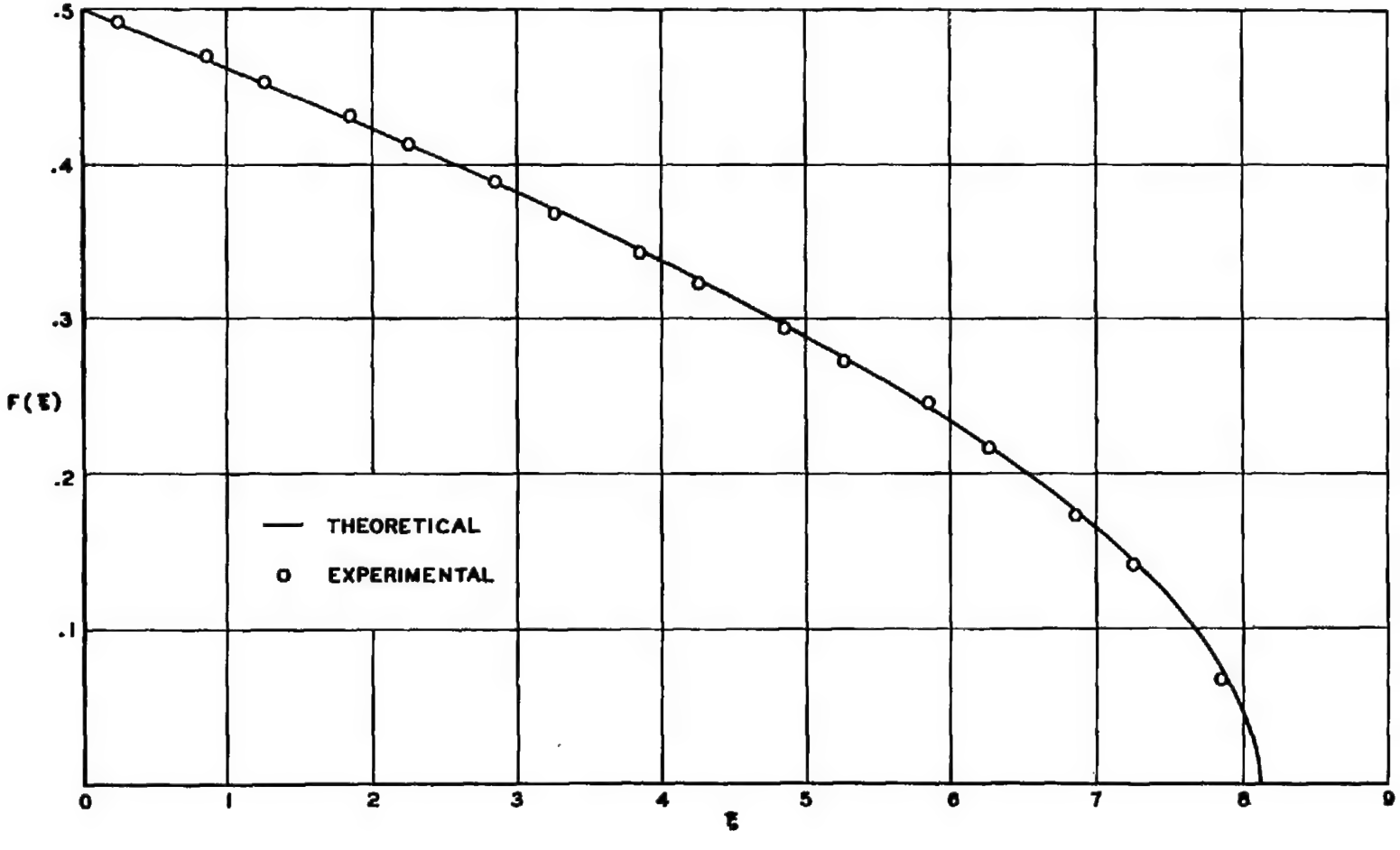

Figure 12.- Distribution function for a sine wave.

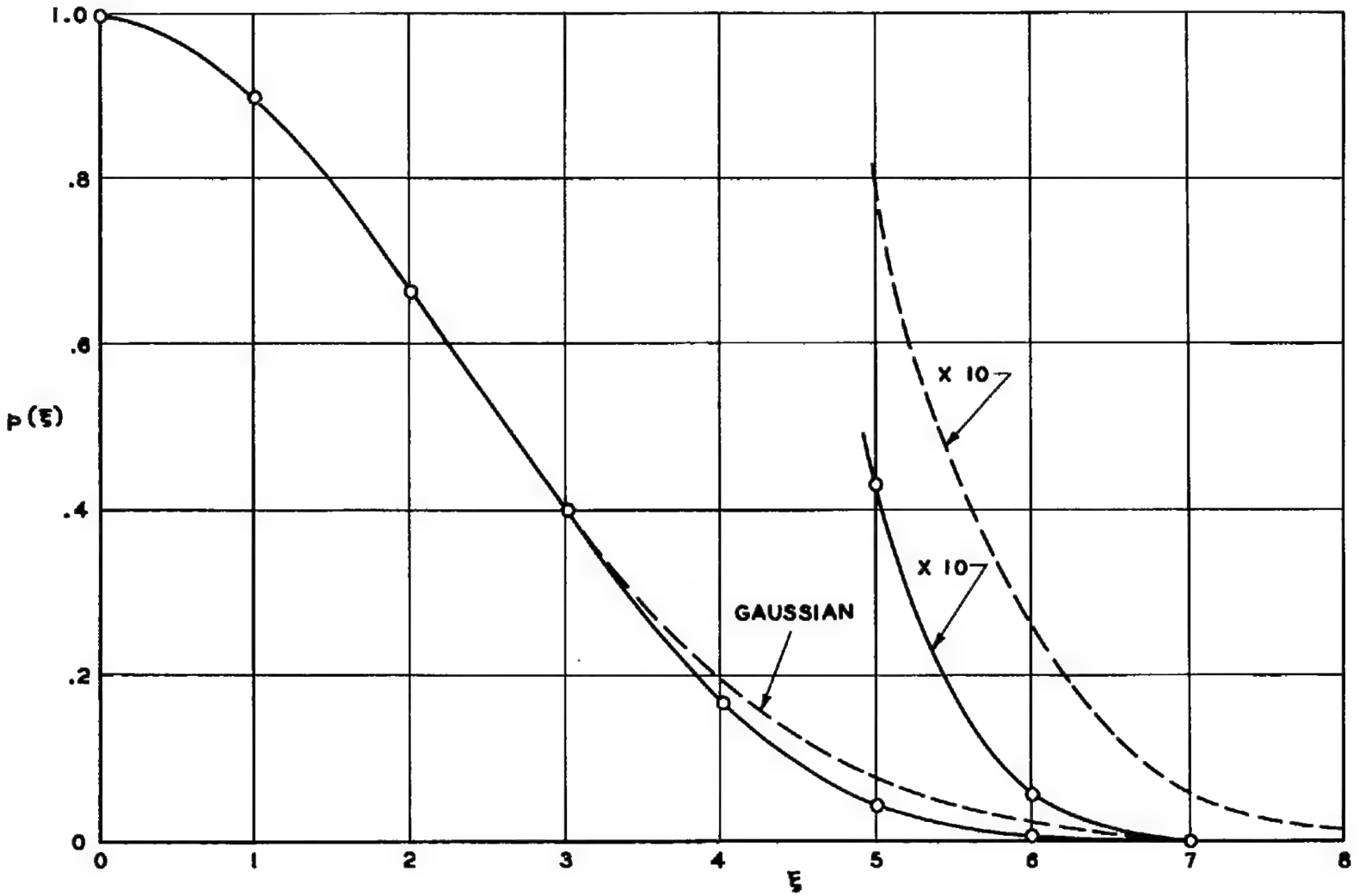

Figure 13.- Distribution of u in isotropic turbulence (corrected for gap width). R_M = 8,100, X/M = 62; C = $0.9\sqrt{\pi/2}$, S = 0.002, f = 2.56.

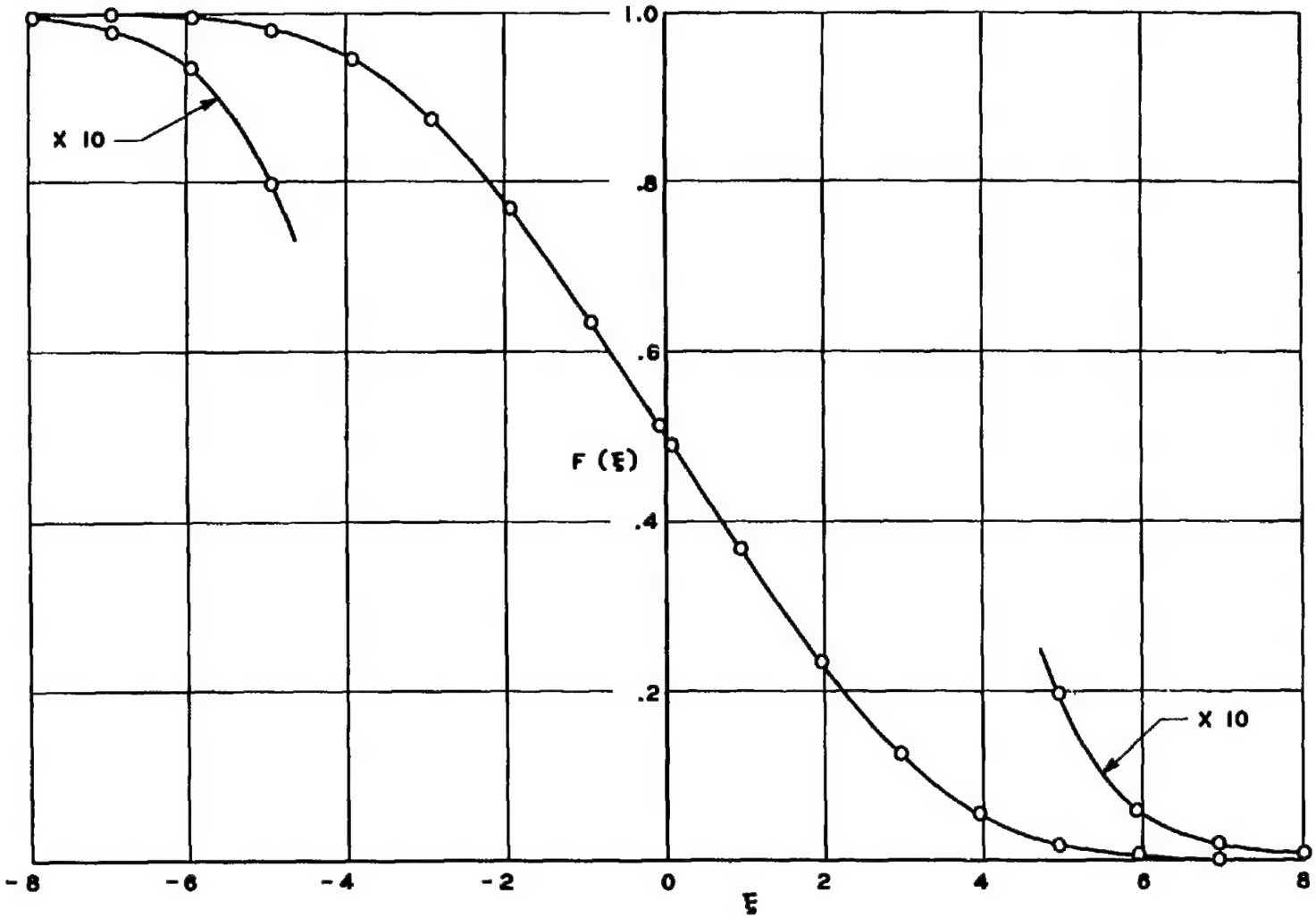

Figure 14.- Distribution function for u(t) in isotropic turbulence. R_M = 11,000, X/M = 50, M = 1.68 centimeters; C = $0.980\sqrt{\pi/2}$, S = 0.006, f = 2.73.

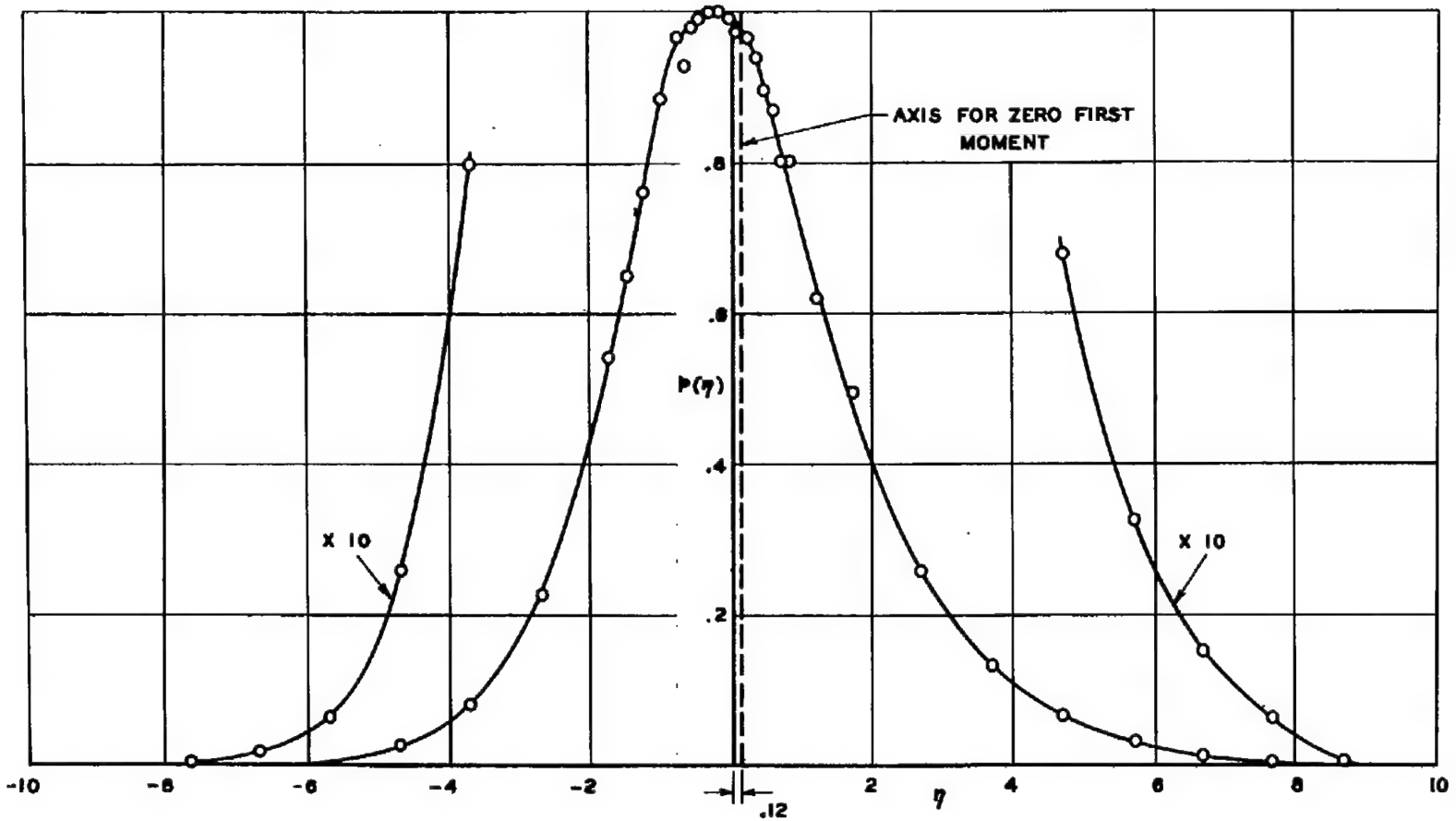

Figure 15.- Distribution of du/dt in isotropic turbulence. $R_M = 8{,}100$, $X/M = 62$; $C = 1.02\sqrt{\pi/2}$, $S = -0.42$, $f = 3.76$.

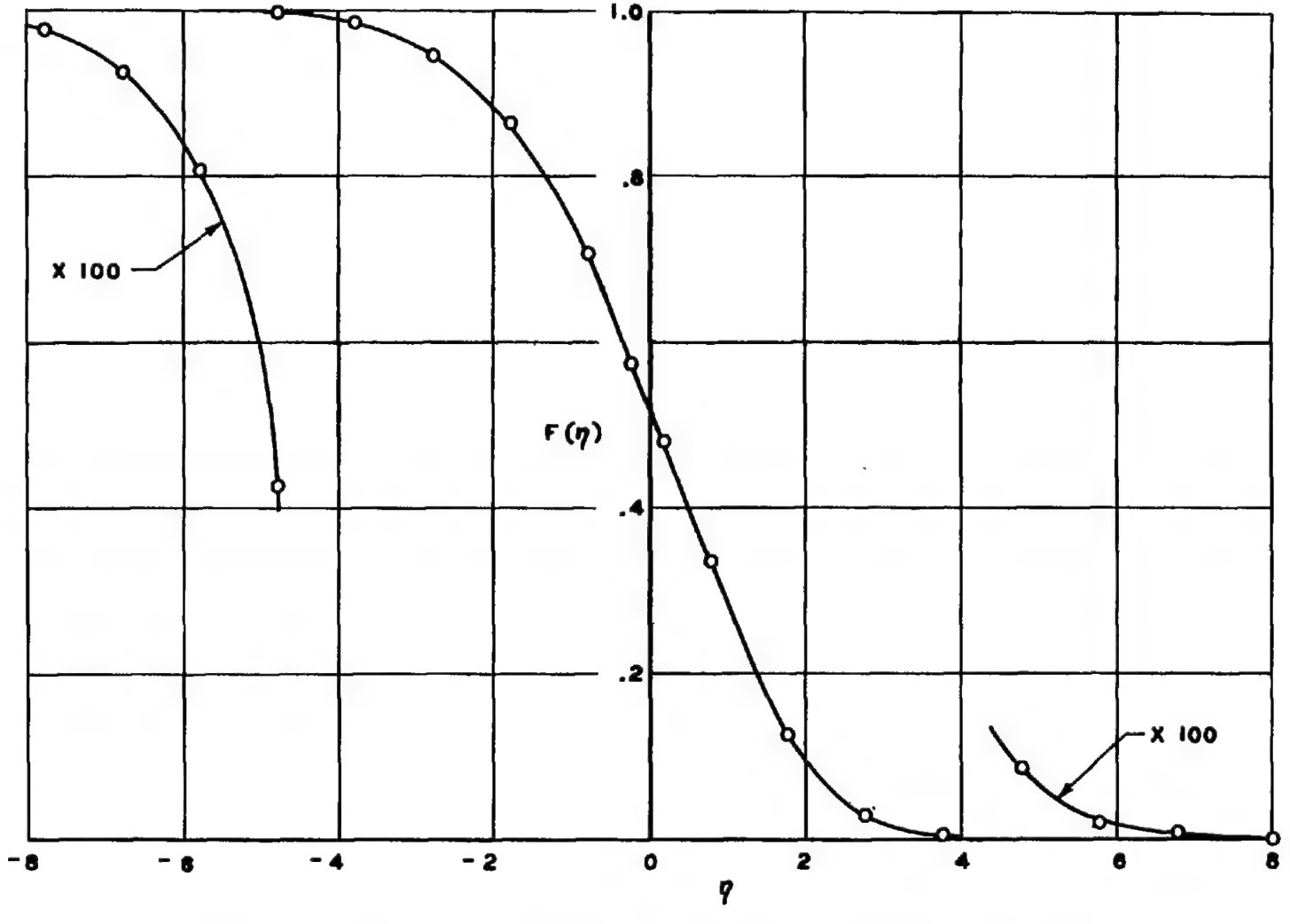

Figure 16.- Distribution function for du/dt in isotropic turbulence. $R_M = 11{,}000$, $X/M = 50$, $M = 1.68$ centimeters; $C = 0.984\sqrt{\pi/2}$, $S = -0.439$, $f = 3.80$.

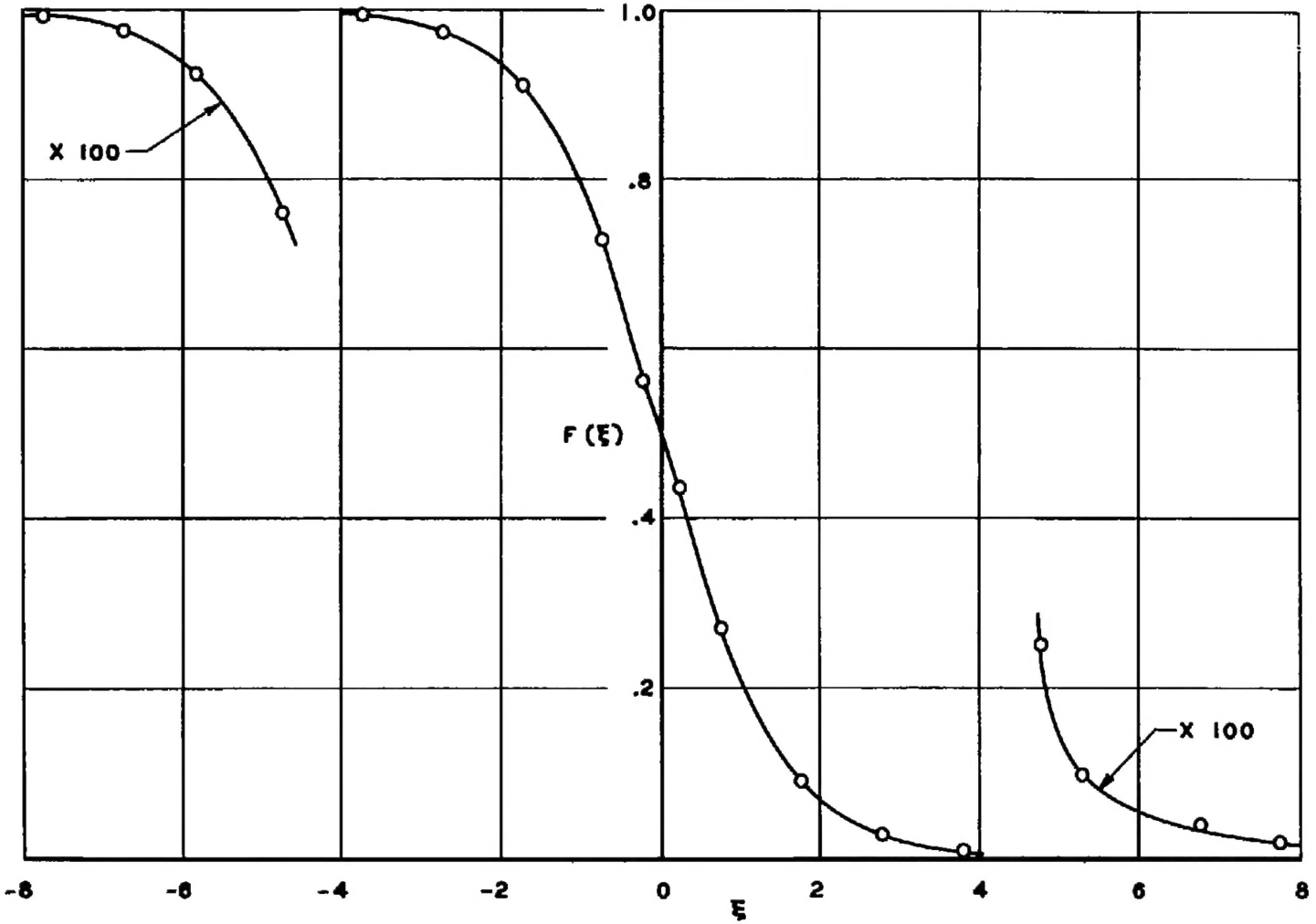

Figure 17.- Distribution function for d^2u/dt^2 in isotropic turbulence. R_M = 11,000, X/M = 50, M = 1.68 centimeters; $C = 1.04\sqrt{\pi/2}$, S = 0.031, f = 4.59.

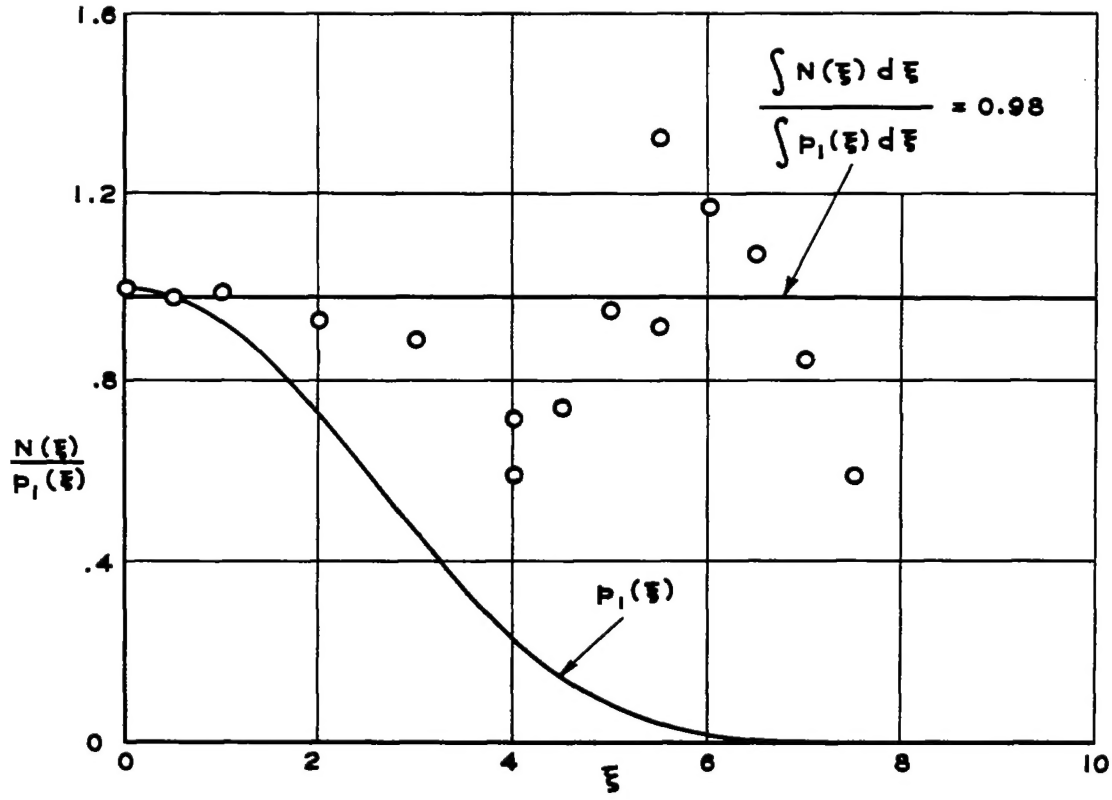

Figure 18.- Plot of $N(\xi)/P_1(\xi)$.

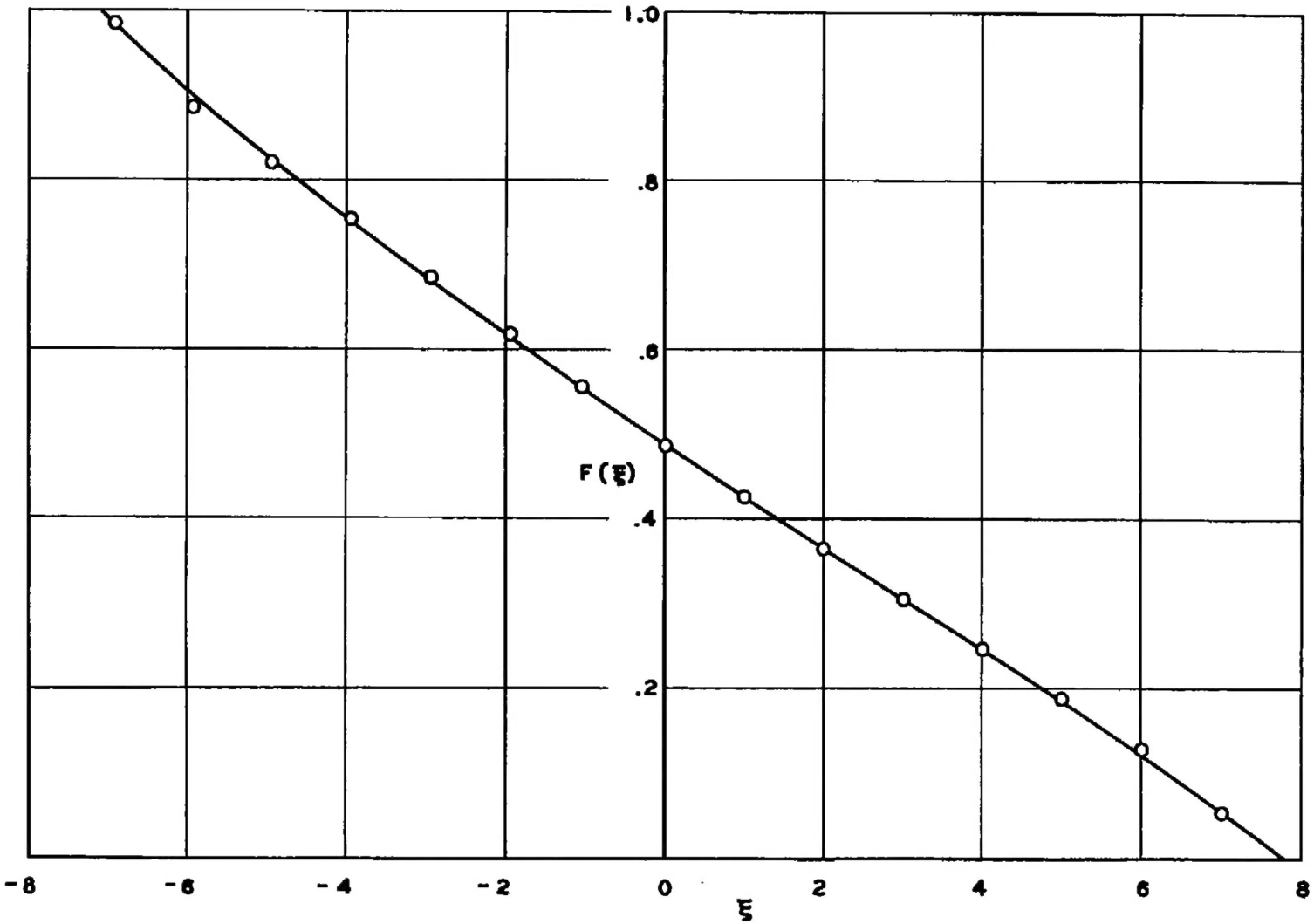

Figure 19.- Distribution function for $u(t)$ in vortex street behind circular cylinder of diameter d at a Reynolds number $R = 100$. $X/d = 6$, $Y/d = 1.3$; $C = 1.15$, $S = 0.08$, $f = 1.7$.

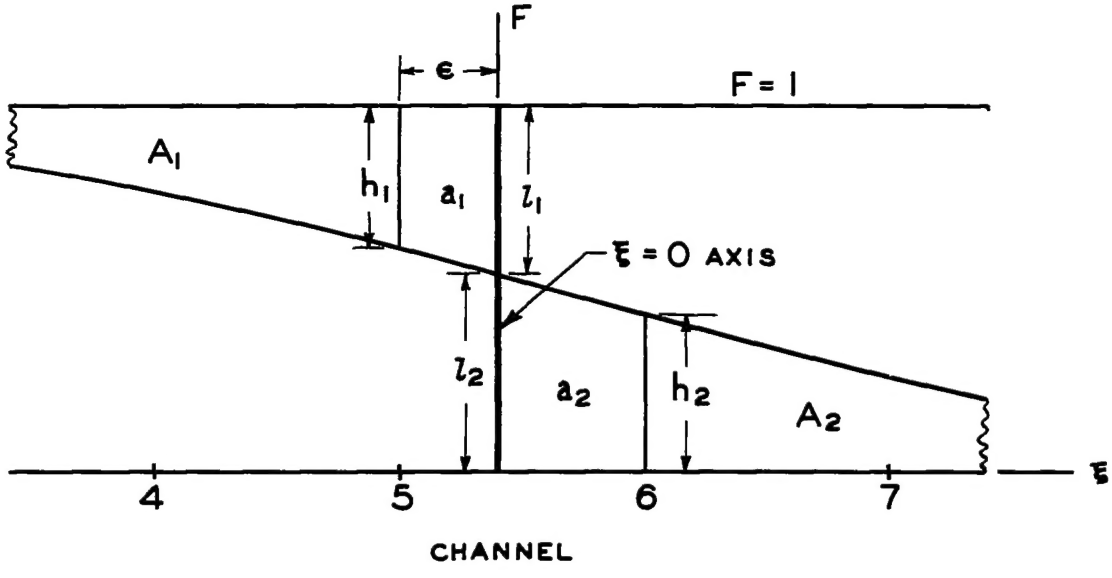

Figure 20.- Calculation of $\xi = 0$ axis. A_1, A_2, a_1, a_2, areas; l_1, l_2, h_1, h_2, ϵ, lengths.